The Partition of Stresses in Al-Si-based Metal-Matrix Composites

T.R. Finlayson[a], J.R. Griffiths[b], D.M. Viano[b], M.E. Fitzpatrick[c], E.C. Oliver[d] and Q.G. Wang[e]

[a] *School of Physics, The University of Melbourne, Parkville, Victoria. 3010*
[b] *CSIRO Manufacturing & Materials Technology, Pullenvale, Queensland. 4069*
[c] *The Open University, Milton Keynes, MK7 6AA, U.K.*
[d] *CCLRC Rutherford Appleton Laboratory, Didcot, OX11 0QX, U.K.*
[e] *General Motors, Powertrain Materials Engineering, Pontiac, MI 48340-2920, U.S.A.*

Neutron diffraction methods have been used to measure the strains (and hence stresses) in the eutectic Si particles and the Al matrix of an Al-7Si-0.4Mg casting, as functions of the applied tensile strain, Three components of stress have been identified: (i) the thermal misfit stress; (ii) the elastic misfit stress; and (iii) the plasticity misfit stress.

1. Introduction

Al-7Si-0.4Mg is a widely used casting alloy. The microstructure, in our case, (Fig. 1) comprises (i) dendrite colonies or grains with a diameter of ~0.8 mm, (ii) Al dendrites with secondary dendrite arm spacings (SDASs) ranging from 20μm to 70 μm and (iii) a eutectic of micron-sized Si particles and Al. During tensile straining the Si particles cleave, the number of broken particles increasing with strain until complete fracture of the alloy occurs at between 3% and 12% strain [1]. The ductility increases with decreasing SDAS.

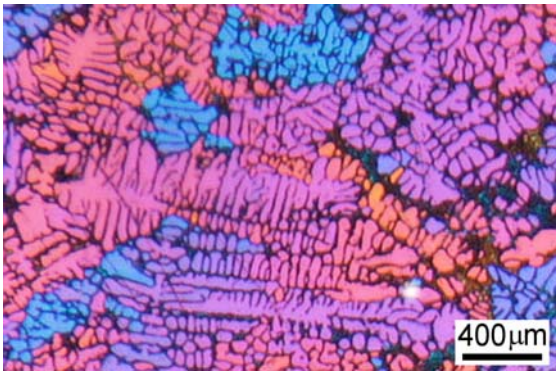

1a

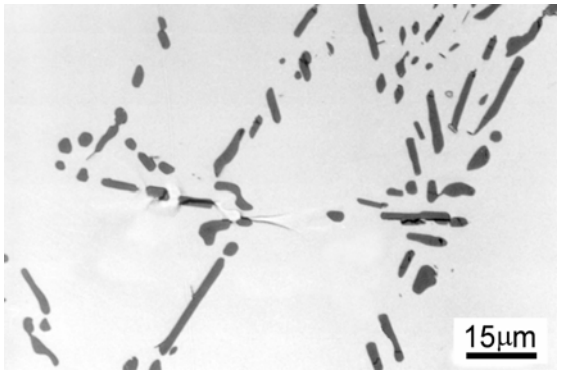

1b

Fig. 1: Microstructure of the casting. (1a) is photographed under polarized light in which individual colonies show as different colours; (1b) shows arrays of Si particles between dendrite arms.

Controversy exists concerning (a) the fracture strength of the Si particles [2,3] and (b) how they contribute to the yield stress and work-hardening rate of the alloy [4,5]. These controversies centre on estimates of the partitioning of stress between the Al matrix and the Si particles, on which there is almost no reliable experimental information.

The aim of this research is to provide such information.

2. Experimental details

Plates (140 x 160 x 25 mm) of nominal composition (wt%) Al-6.6Si-0.4Mg were sand-cast in moulds having a large chill at one end to produce a range of SDASs from 20 μm at the chill end to 70 μm at the other end. Slices were cut from either end of the plates and solution

heat-treated at 540°C for 6 hours followed by a cold water quench (condition T4). A second microstructural condition (T6) involved aging for 6 hours at 170°C. Tensile specimens with a parallel gauge length of 20 mm and a diameter of 8 mm were then machined from the slices.

In-situ neutron diffraction lattice strain measurements were made during tensile testing using the ENGIN-X instrument at the ISIS pulsed source. The instrument has two fixed-angle detector banks centered on scattering angles of ±90°. The detectors measure time-resolved diffraction patterns corresponding to scattering vectors aligned at ±45° to the incident beam with a timing window set to detect interplanar spacings in the range $0.076 \leq d_{hkl} \leq 0.24$ nm. The load axis was at 45° to the incident beam allowing simultaneous measurements of lattice strains parallel and perpendicular to the applied load. The diffraction patterns were analyzed by Rietveld refinement. "Zero strain" lattice parameters were measured using NIST standard Si powder (lattice parameter, $a_0 = 0.543119$ nm) and powders made by filing alloys following the T4 and T6 treatments, both of which gave $a_0 = 0.404921$ nm for the Al phase.

3. Results and Discussion

3.1 Thermal Misfit Stresses

Measured lattice parameters as functions of applied stress (less than yield) were used to derive the lattice parameters for both the Si and the Al matrix phases at zero applied stress, since the initial diffraction pattern for each sample was collected with the sample positioned on the testing machine but at a very low applied stress (~ 10 MPa). These extrapolations (for, say, a T6 sample) gave (for Si) 0.542784 nm and 0.542722 nm for the axial and transverse measurements, respectively, and (for the Al matrix) 0.404992 nm and 0.404966, indicating, as expected from the relative thermal expansion coefficients, that the Si phase is under an hydrostatic compressive strain of -617×10^{-6} and the Al matrix an hydrostatic tensile strain of 143×10^{-6}. Using values of 162 GPa and 0.22 for the Young's modulus and Poisson's ratio (for Si) and 70 GPa and 0.34 for Al [6], these strains converted to stresses of -180 MPa in the Si particles and +29 MPa in the Al matrix.

The volume fraction of Si particles is 0.0757 so the net stress is (- 13.6 + 26.6) MPa, implying a violation of stress equilibrium of 13 MPa. Comparable small imbalances were found for all samples measured.

Application of the Eshelby theory [7] predicts a thermal misfit stress in the Si particles of 1.5 MPa/°C so that the value of -180 MPa suggests a temperature difference of 120°C, smaller than that which is experienced during the material processing. A likely explanation for this observation is stress relaxation during cooling.

3.2 Elastic Misfit Stresses

These arise in a composite under load because of differences in the elastic constants of the phases. From measured lattice constants in the elastic regime, strains (and hence stresses) in the phases were determined. For a T6 sample, for example, these were 1.28 MPa per MPa applied, in the Si particles and 0.93 per MPa in the Al matrix (see Fig.2). Using $(V_f\sigma_{Si} + (1 - V_f)\sigma_{Al} - 1)$, where the σs are the measured misfit stresses and V_f is the volume fraction of Si particles, the stress equilibrium violation at an applied stress

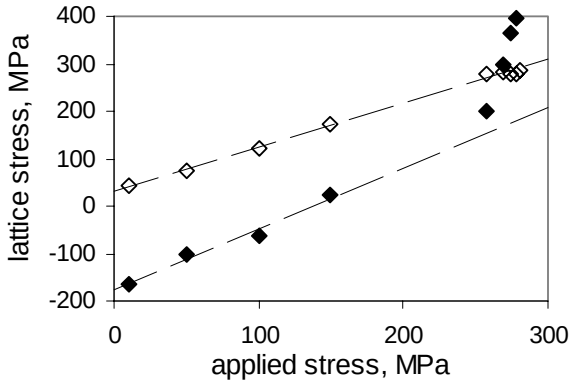

Fig. 2. Axial stresses in the Si particles (solid symbols) and Al matrix (open symbols) as the specimen is loaded (T6, fine SDAS). Dashed lines show the elastic regime.

of 1 MPa is -0.044 MPa (that is, an error of 4.4%). Eshelby theory [7] predicts elastic stresses of 1.27 MPa in the Si per MPa applied and 0.98 MPa in the Al matrix, in reasonable agreement with the measured data, although it is emphasized that the microstructures of the present composites are more complex than can be treated by Eshelby theory.

3.3 Plasticity Misfit Stress

This arises when the Al matrix begins to flow around the Si particles. Its onset is evident in Fig. 2 in which the axial stresses in the Si particles and Al matrix are plotted as the specimen is loaded beyond yield, by departures from the dashed elastic lines. Unfortunately, it is not possible to extract the plasticity contribution from the data except at high plastic strains as explained below. The apparently obvious assumption that $\sigma_{total} = \sigma_{thermal} + \sigma_{elastic} + \sigma_{plastic}$ is invalid. This is because the $\sigma_{thermal}$ term is not constant. It is a function of the plastic strain, reducing from its full initial value at a plastic strain of zero (i.e., for all applied stresses up to and including yield) to almost zero at a plastic strain of 1% or 2% [8]. This problem was not appreciated by us in our earlier work [9] and a full numerical stress analysis is in the process of being carried out for a future publication.

3.4 The Fracture Strength of the Si Particles

Si particles, particularly larger ones, begin to fracture at a plastic strain of ~ 0.01 [1] at which σ_{total} is in the range 300 – 330 MPa for T6 and 200 – 220 MPa for T4 material. These give a lower limit to the particle strength, and this is considerably less than the 500 – 3500 MPa suggested from earlier work involving Weibull analysis of data following mechanical testing and optical observations of cracked particles [5]. Future experiments are planned, particularly involving compression testing for which this initial particle cracking will not be an issue.

Acknowledgments

We acknowledge CCLRC for access to ENGIN-X and General Motors R&D for the cast plates. TRF, JRG and DV acknowledge support from the Access to Major Research Facilities Programme, a component of the International Science Linkages Programme under the Australian Government's innovation statement, Backing Australia's Ability.

References

[1] C.H. Cáceres, C.J. Davidson, J.R. Griffiths and Q.G. Wang, *Metall. Mater. Trans.* **30A,** 2611 (1999).
[2] J. Campbell, *Mater. Sci. & Technol.* **22**, 127 (2006).
[3] J.R. Griffiths, *Mater. Sci. & Technol.* **22**, 1001 (2006).
[4] A.A. Benzerga, S.S. Hong, K.S. Kim, A. Needleman and E. van der Giessen, *Acta Mater.* **49**, 3071 (2001).
[5] C.H. Cáceres and J.R. Griffiths, *Acta Mater.* **44**, 25 (1996).
[6] V.A. Lubarda, *Mechanics of Materials*, **35**, 53 (2003).
[7] T.W. Clyne and P.J. Withers, *An Introduction to Metal Matrix Composites*, (Cambridge University Press, 1993).
[8] J. LLorca, A. Martin, J. Ruiz and M. Elices, *Metall. Trans.* **24A**, 1575 (1993).
[9] T.R. Finlayson, J.R. Griffiths, D.M. Viano, M.E. Fitzpatrick, E.C. Oliver and Q.G. Wang, in *Shape Casting: The Second Int. Symposium*, eds. P N Crepeau, M Tiryakioglu, J Campbell, TMS (The Minerals, Metals and Materials Society), p.127 (2007).